Simultaneous Measurement of Electric Birefringence and Dichroism. A Study on Photosystem 1 Particles

Bart van Haeringen, Jan P. Dekker, Michael Bloemendal,* Matthias Rögner,‡ Rienk van Grondelle, and Herbert van Amerongen

Department of Biophysics, Free University and Institute for Molecular Biological Sciences, 1081 HV Amsterdam, The Netherlands; *Department of Protein and Molecular Biology, Royal Free Hospital School of Medicine, London NW3 2PF, England; and ‡Institute of Botany, University of Münster, D-48149 Münster, Germany

ABSTRACT We have developed a straightforward method to separate linear-dichroism and birefringence contributions to electric-field induced signals in a conventional birefringence setup. The method requires the measurement of electric birefringence for three different angular positions of the analyzer. It is demonstrated that the presence of linear dichroism can significantly influence the measured signals and lead to completely erroneous calculations of the birefringence signal and field-free decay times if its contribution is not taken into account. The new method is used to determine electric birefringence and linear dichroism of trimeric Photosystem 1 complexes from the cyanobacterium *Synechocystis* PCC 6803 in the detergents *n*-dodecyl-β-D-maltoside and *n*-octyl-β-D-glucoside. It is concluded that the orientation of the particles in the field is predominantly caused by a permanent electric dipole moment that is directed parallel to the symmetry axis of the particles. Comparison of the decay times obtained with dodecylmaltoside and octylglucoside supports a model in which the thickness of the disc-like complexes remains similar (7–8 nm) upon replacing dodecylmaltoside by octylglucoside, whereas the diameter increases from 14.4 ± 0.2 to 16.6 ± 0.2 nm because of an increased thickness of the detergent layer. This change in diameter is in good agreement with electron-microscopy results on Photosystem 2 complexes in dodecylmaltoside and octylglucoside (Dekker, J. P., E. J. Boekema, H. T. Witt, and M. Rögner. 1988. *Biochim. Biophys. Acta* 936:307–318). The value of approximately 16.6 nm for the diameter of Photosystem 1 trimers in dodecylmaltoside is in good agreement with recent results obtained from electron microscopy in combination with extensive image analysis (Kruip, J., E.J. Boekema, D. Bald, A. F. Boonstra, and M. Rögner. 1993. *J. Biol. Chem.* 268:23353–23360).

INTRODUCTION

Electric dichroism and electric birefringence have been used successfully to study structural and functional aspects of biological macromolecules in solution (Fredericq and Houssier, 1973; O'Konski, 1978; Krause, 1980; Nordén et al., 1992). These techniques often use a square electric-field pulse to partially orient the molecules (Fredericq and Houssier, 1973). The rise and decay of the orientation process can be monitored via the induced transient electric birefringence (TEB) or the induced transient linear dichroism (LD). From the amplitudes of the birefringence and dichroism as a function of the applied electric-field strength, several electro-optical quantities can be obtained. The rate of the field-free decay is directly related to the rotational diffusion constants of the molecules under study (Fredericq and Houssier, 1973). Because rotational motion is much more responsive to size and shape than translational motion, these methods yield more accurate information on molecular shape and dimensions than methods that are based on the detection of translational motion like centrifugation (Garcia de la Torre and Bloomfield, 1981). In combination with the large time window available, this allows for example the simultaneous study of single molecules and their aggregates in solution (Van Haeringen et al., 1992).

It is straightforward to perform LD measurements in such a way that birefringence does not contribute to the signals. The reverse is not true, and methods to determine birefringence in absorption bands have so far required the separate measurement of the LD to eliminate its contribution to the birefringence signals and to determine unambiguously the sign of the LD contribution (Yamaoka and Charney, 1973; Ravey, 1976; Tricot and Houssier, 1976). In this study, we present a relatively simple method to separate birefringence and LD contributions to signals obtained in a conventional birefringence setup. We demonstrate how the presence of LD can significantly influence the determined values for birefringence and its field-free decay times if the LD contribution is neglected. Thereafter, we apply the new method to determine the birefringence and LD transients of trimeric Photosystem 1 (PS1) complexes from the cyanobacterium *Synechocystis*. PS1 trimers are photosynthetic membrane proteins that have well been characterized by electron microscopy in combination with extensive image analysis (Boekema et al., 1994). The particles appear to be disc-like shaped, with a thickness of 6–9 nm (depending on protein composition) and a diameter of approximately 19 nm. Trimeric PS1 needs detergents to stay solubilized, and it is to be expected that the size of the detergent molecules contributes to the diameter of the total particle (Dekker et al., 1988). Therefore, we measured the electric birefringence of PS1 trimers using *n*-dodecyl-β-D-maltoside and *n*-octyl-β-D-glucoside. The exponential decay times of the birefringence signals were used to determine the approximate dimensions of the complexes in both detergents. Comparison of the electric LD and the LD from measurements on compressed gels (Van der Lee et al., 1993) allowed the deter-

Received for publication 1 March 1994 and in final form 29 April 1994.

0006-3495/94/07/411/07 $2.00

mination of the orientation of the predominant electric dipole moment that contributes to the orientation of the particles in the electric field.

MATERIALS AND METHODS

Trimeric PS1 particles were prepared from *Synechocystis* sp. PCC 6803 as described by Rögner et al. (1990). By means of a Pharmacia PD-10 column, the preparations were brought into a buffer of low ionic strength necessary for TEB experiments (1.0 mM 2-[*N*-morpholino]ethane-sulfonic acid (MES), 0.5 mM $MgCl_2$, 0.5 mM $CaCl_2$, 0.06% *n*-dodecyl-β-D-maltoside (DM), pH 6.5). Some experiments were performed on buffers containing *n*-octyl-β-D-glucoside (OGP) (1.0 mM MES, 0.5 mM $MgCl_2$, 0.5 mM $CaCl_2$, 1.2% OGP, pH 6.5). Starting from the solutions containing DM, buffers were exchanged with the use of an anion-exchange column (Mono-Q, Pharmacia, Uppsala, Sweden).

TEB-measurements were performed as described previously (Van Haeringen et al., 1992). The emission line of the Argon ion laser was set at 488.0 nm with a power of less than 5 mW impinging on the sample. It was checked by absorption measurements that no laser-induced particle damage occurred during the experiments. To sustain the integrity of the sample, the light beam was blocked between pulses by means of a shutter. The measurements were performed at a sample temperature between 4 and 20 °C and an optical density of the sample in the measuring cell at 488.0 nm of about 1.0. The pulse duration was varied over 6–25 μs, the field strength was 1.5–11.0 kV/cm. For each average birefringence curve, at least 20 transients were collected. The field-free decays of the signals were fitted to a sum of exponential relaxation times using the computer program DISCRETE (Provencher, 1976a, b). Amino acid sequences of PS1 proteins were retrieved from the EMBL gene bank and subsequently analyzed with the HUSAR software package, based at the DKFZ (Heidelberg, Germany).

THEORY

This section assumes a birefringence setup that makes use of a quarter-wave plate with its slow axis at an angle of $3\pi/4$ relative to the direction of the electric field. The advantages of such a configuration have been discussed in detail by Fredericq and Houssier (1973). Fig. 1 *A* shows the main components of the system; Fig. 1 *B* shows a schematic cross section of the optical configuration viewed along the optical axis in the direction of the propagating light. When in the presence of an orienting electric field, the sample becomes birefringent and dichroic, the electric field component of the light emerging from the Kerr-cell can be decomposed into two components, one directed parallel to the applied electric field ($E_\parallel$) and the other perpendicular to the field ($E_\perp$):

$$E_\parallel = \tfrac{1}{2}\sqrt{2}E_0 10^{-A_\parallel/2}\sin(\omega t - \delta) \quad (1)$$

$$E_\perp = \tfrac{1}{2}\sqrt{2}E_0 10^{-A_\perp/2}\sin(\omega t), \quad (2)$$

where E_0 is the amplitude and ω is the angular frequency

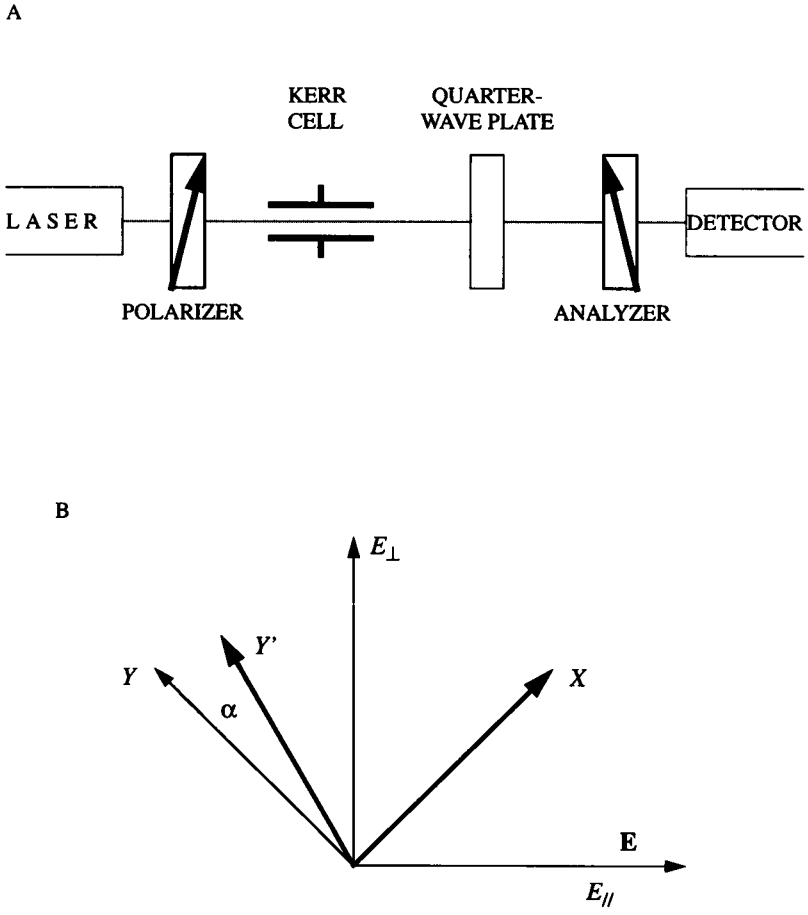

FIGURE 1 Schematic views of the optical part of the electric birefringence setup. (*A*) An upper view of the different components. (*B*) Cross section using an arrangement with the λ/4 waveplate having its slow axis *Y* at $3\pi/4$ with respect to the electric-field direction **E**. *X* and *Y'* denote de orientations of the polarizer and analyzer, respectively. α is the angle over which the analyzer is rotated from the crossed position, $E_\parallel$ and $E_\perp$ denote the electric-field components of light parallel and perpendicular to **E**, respectively.

of the lightwave, $A_\parallel$ and $A_\perp$ are the absorptions of the sample for light with its polarization directed parallel and perpendicular to the electric field, respectively, and δ is the optical retardation that $E_\parallel$ undergoes (relative to $E_\perp$) because of induced birefringence.

The light falls on the quarter-wave plate and can be rewritten in components along the fast (E_X) and slow axes of the quarter-wave plate (E_Y):

$$E_X = \tfrac{1}{2}\sqrt{2}(E_\perp + E_\parallel) = \tfrac{1}{2}E_0(10^{-A_\perp/2}\sin\omega t + 10^{-A_\parallel/2}\sin(\omega t - \delta)) \quad (3)$$

$$E_Y = \tfrac{1}{2}\sqrt{2}(E_\perp - E_\parallel) = \tfrac{1}{2}E_0(10^{-A_\perp/2}\sin\omega t - 10^{-A_\parallel/2}\sin(\omega t - \delta)). \quad (4)$$

After the quarter-wave plate E_Y is delayed $\pi/2$ in phase with respect to E_X. For the emerging beams with electric field components E'_X and E'_Y we obtain

$$E'_X = E_X \quad (5)$$

$$E'_Y = \frac{1}{2}E_0\left(10^{-A_\perp/2}\sin\left(\omega t - \frac{\pi}{2}\right) - 10^{-A_\parallel/2} \cdot \left(\sin\left(\omega t - \frac{\pi}{2}\right)\cos\delta - \cos\left(\omega t - \frac{\pi}{2}\right)\sin\delta\right)\right). \quad (6)$$

The light transmitted by the analyzer ($E_{Y'}$), which is rotated over an angle α from the crossed position, can now be written as

$$E_{Y'} = E'_Y\cos\alpha + E'_X\sin\alpha, \quad (7)$$

and after some goniometric manipulation

$$E_{Y'} = B\sin(\omega t + \alpha) + C\cos(\omega t + \alpha), \quad (8)$$

with

$$B = \tfrac{1}{2}E_0 10^{-A_\parallel/2}\sin(2\alpha + \delta) \quad (9)$$

$$C = \tfrac{1}{2}E_0(-10^{-A_\perp/2} + 10^{-A_\parallel/2}\cos(2\alpha + \delta)) \quad (10)$$

To rewrite Eq. 8 to a form that contains only a single oscillatory term, we define

$$\cos\delta' = \frac{B}{\sqrt{B^2 + C^2}} \quad (11)$$

and

$$\sin\delta' = \frac{C}{\sqrt{B^2 + C^2}}. \quad (12)$$

Then,

$$E_{Y'} = \sqrt{B^2 + C^2}\sin(\omega t + \alpha + \delta'). \quad (13)$$

For the intensity of the light that reaches the detector because of the electric-field induced birefringence and dichroism, and for the analyzer rotated over an angle α from the crossed position, the following relation holds:

$$I_\alpha(E) = B^2 + C^2 = \tfrac{1}{4}E_0^2(10^{-A_\parallel} + 10^{-A_\perp}) - \tfrac{1}{2}E_0^2\cos(2\alpha + \delta)10^{-(1/2)(A_\parallel + A_\perp)}. \quad (14)$$

$I_\alpha(0)$ (transmitted light intensity in the absence of electric birefringence and dichroism, for the analyzer rotated over an angle of α from the crossed position) is given by

$$I_\alpha(0) = E_0^2 10^{-A}\sin^2\alpha = \kappa\sin^2\alpha, \quad (15)$$

with A the isotropic absorption. The proportionality constant κ can be determined experimentally from a plot of $I_\alpha(0)$ vs. $\sin^2\alpha$. Such a plot is also used as a check for the linear response of the birefringence apparatus.

From

$$\Delta A = A_\parallel - A_\perp, \quad (16)$$

and

$$3A = A_\parallel + 2A_\perp, \quad (17)$$

it follows that

$$\frac{I_\alpha(E)}{\kappa} = \left(\frac{1}{4}10^{-(2/3)\Delta A} + \frac{1}{4}10^{+(1/3)\Delta A} - \frac{1}{2}10^{-(1/6)\Delta A} + 10^{-(1/6)\Delta A}\sin^2\left(\alpha + \frac{\delta}{2}\right)\right). \quad (18)$$

The parameter Z is now defined as

$$Z = \frac{I_\alpha(E) - \kappa\sin^2\alpha}{\kappa} = \frac{I_\alpha(E) - I_\alpha(0)}{\kappa}. \quad (19)$$

Z represents the fractional change in light intensity transmitted by the analyzer due to the induced dichroism and birefringence. In the absence of dichroism ($\Delta A = 0$), for instance when a measurement is performed in a spectral region where the absorption of the sample is zero, $Z/\sin^2\alpha$ reduces to the conventional expression for the calculation of δ (Fredericq and Houssier, 1973).

Z is determined experimentally and can be expressed in terms of birefringence (δ) and dichroism (ΔA) according to

$$Z = \tfrac{1}{4}10^{-(2/3)\Delta A} + \tfrac{1}{4}10^{+(1/3)\Delta A} - \tfrac{1}{2}10^{-(1/6)\Delta A} + 10^{-(1/6)\Delta A}\sin^2\left(\alpha + \frac{\delta}{2}\right) - \sin^2\alpha. \quad (20)$$

The ΔA and δ terms can now be separated by measuring Z for three values of α, namely, $Z(0)$, $Z(\alpha)$, and $Z(-\alpha)$. By expanding $\sin^2(\alpha + \delta/2)$ it can be shown that

$$Q_1 = \frac{Z(\alpha) + Z(-\alpha)}{\sin 2\alpha} = 10^{-(1/6)\Delta A}\sin\delta \quad (21)$$

and

$$Q_2 = Z(\alpha) + Z(-\alpha) - 2Z(0) + 2\sin^2\alpha = 10^{-(1/6)\Delta A}(1 - \cos 2\alpha)\cos\delta, \quad (22)$$

from which another simple manipulation yields

$$\tan \delta = \frac{Q_1}{Q_2}(1 - \cos 2\alpha) = \frac{\tan \alpha}{Q_2}(Z(\alpha) - Z(-\alpha)). \quad (23)$$

The right-hand side of Eq. 23 is completely experimentally determined in terms of the basic measurements of Z. ΔA can be determined from Eqs. 21 and 22, once δ is known.

In general the time-dependent behavior of the birefringence and LD is of particular interest. When the above procedure is applied for Z as a function of time t, both the time-resolved birefringence $\delta(t)$ and linear dichroism $\Delta A(t)$ curves can be obtained. This calculation requires the manipulation of three sets of data arrays obtained with the same experimental conditions, with the only independent variable the variation in the analyzer angle α. Although it is necessary to measure Z for three values of α, it is generally better if more measurements and a least-squares analysis is performed.

Thus, by measuring the Z-curves for three angular positions of the analyzer but, further, under the same experimental conditions, both the time-resolved birefringence and linear-dichroism traces can be recovered.

RESULTS AND DISCUSSION

The effect of electric dichroism on birefringence results

The relevant quantities to be obtained from TEB-experiments are the amplitude (δ) and the field-free relaxation time (τ) of the electric-field induced birefringence. The former allows, as a function of the orienting electric-field strength, the calculation of several electro-optical quantities, whereas the latter is directly related to the rotational diffusion coefficients of the molecules under study (Fredericq and Houssier, 1973). We will now demonstrate that determination of the birefringence can lead to completely erroneous results for both the values of δ and τ, if the contribution of LD is neglected.

Fig. 2 *A* illustrates the relative error made in the calculation of $\delta(\alpha)$ when the contribution of linear dichroism is not taken into account. δ denotes the real value for the birefringence, whereas δ' denotes the one determined from the hypothetical experiment without correcting for LD. From Eqs. 18 and 20, it follows that $\delta'(\alpha)$ can be calculated as

$$\delta'(\alpha) = 2 \operatorname{asin}\sqrt{(Z(\alpha) + \sin^2 \alpha)} - 2\alpha, \quad (24)$$

which is the expression that is normally applied to calculate birefringence. In the absence of dichroism ($\Delta A = 0$), it yields the true value of $\delta(\alpha)$. $Z(\alpha)$ can be calculated from Eq. 20. In Fig. 2 *A*, results from calculations for positive δ and α are shown. For $\delta > 0$ and $\alpha < 0$, and for $\delta < 0$ for both $\alpha < 0$ and $\alpha > 0$, comparable results are obtained. It is obvious that the error made in the calculation of δ can be considerable when the contribution of LD is ignored.

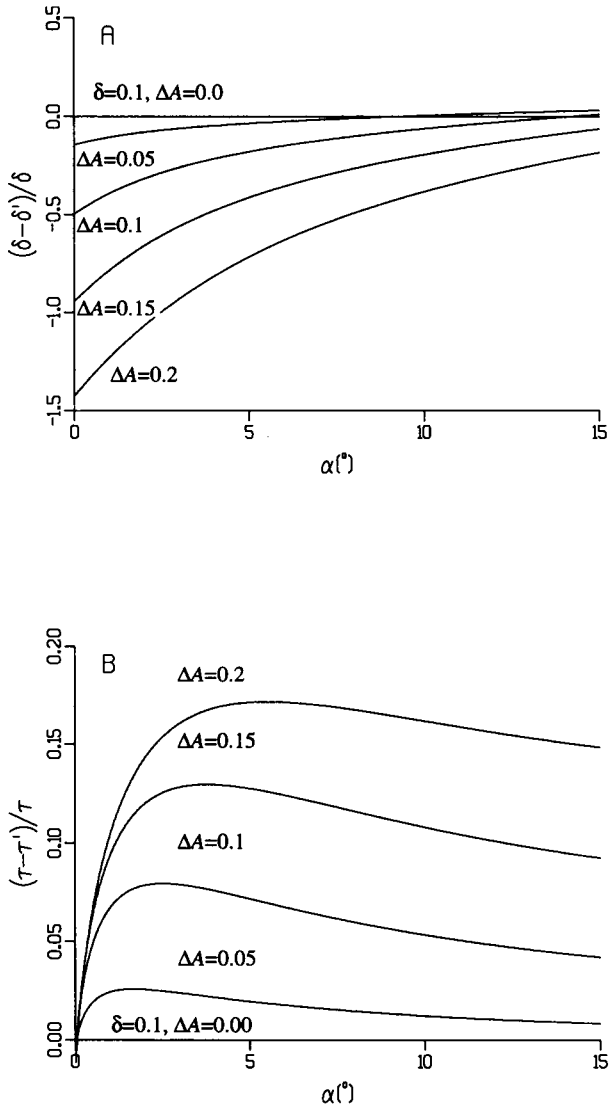

FIGURE 2 Relative errors made in the calculation of the amplitude δ and the average field-free relaxation time τ of the birefringence using simulated data (see text). δ and τ denote the true values, δ' and τ' the calculated ones for fixed δ and different values of ΔA ($\delta = 0.1$ and $\Delta A = 0.00$, 0.05, 0.10, 0.15, and 0.20).

Fig. 2 *B* shows some examples of the relative error made in the calculation of $\tau(\alpha)$ when the contribution of linear dichroism is not taken into account. τ denotes an arbitrarily chosen monoexponential relaxation time of the true birefringence δ, whereas τ' denotes the relaxation time of δ'. $\tau'(\alpha)$ was calculated from

$$\tau'(\alpha) = \int_0^\infty \delta'(\alpha, t)\, dt, \quad (25)$$

with δ' given by Eq. 24 and $t = 0$ corresponding to the moment that the electric field is switched off. In the absence of dichroism ($\Delta A = 0$), Eq. 25 gives the relaxation time of the true birefringence δ. In Fig. 2 *B*, results from calculations for positive δ and α are shown. For negative values of δ,

comparable results are obtained for $\alpha < 0$. Errors made in the calculation of τ are generally larger when α and δ are of opposite sign.

From Fig. 2, it follows that the amplitude of the birefringence and its field-free relaxation time strongly depend on α when the contribution of dichroism is ignored in the calculation of the birefringence. In some cases, the errors may be very large. As Fig. 2 shows, errors in δ increase when α decreases, whereas errors in τ are generally smaller when α is diminished. This makes the separation of LD and birefringence of paramount importance. Measuring τ, and in particular δ, as a function of α (under constant experimental conditions) provides a means to detect the presence of linear dichroism in the sample. In the rest of this paper, we will show that the measurement of $Z(\alpha)$ can be used for the separation of the linear-dichroism and birefringence contributions.

Electric birefringence and electric dichroism of PS1 trimers

$Z(\alpha)$ curves of trimeric PS1 in DM containing buffer were experimentally determined from Eq. 19, and further analyzed in terms of δ and ΔA using Eqs. 20–23 as indicated in the Theory section. κ was calculated from the prepulse baselines of $Z(\alpha)$.

Fig. 3 shows the real birefringence (Fig. 3 *A*) and linear dichroism (Fig. 3 *B*) curves at 488 nm, as calculated from Z for $\alpha = 0.00°$ and $\alpha = \pm 7.95°$. From Fig. 3, it appears that the birefringence and linear-dichroism curves have similar shapes (when normalized in amplitude, they practically coincide). In fact, this should be the case when δ and ΔA arise from the same molecules (Fredericq and Houssier, 1973). The buffer is not expected to contribute to the linear-dichroism signal because it does not absorb at 488 nm; however, because of the noise in the LD signal, this is not completely apparent for the linear-dichroism trace shown. The birefringence signal does show a (small) buffer contribution that is opposite in sign to that of the PS1 particle. The steady-state values of the birefringence and linear-dichroism signal shown in Fig. 3 are of similar sign with respective values of approximately -0.040 and -0.075 at 488 nm (sample absorption: 1.0; orienting electric-field strength: 8.5 kV/cm).

A combined analysis of the rise and decay curve of the birefringence according to the area method (Yoshioka and Watanabe, 1969) allows the calculation of the relative contribution of the permanent (P) and induced dipole moment (Q) that contribute to the orientation mechanism. For trimeric PS1 particles, it follows that $P/Q \cong 2.5$, indicating a strong contribution of a permanent dipole moment to the orientation mechanism. Comparison of the electric LD (Fig. 3) with the LD measured in compressed gels (Van der Lee et al., 1993) allows determination of the orientation of the permanent dipole moment in PS1 trimers. The sign of the electric LD is opposite to that of the LD measured in compressed gels (Van der Lee et al., 1993). This means that the

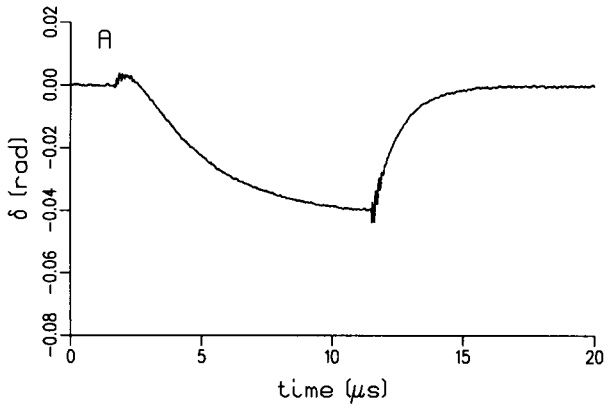

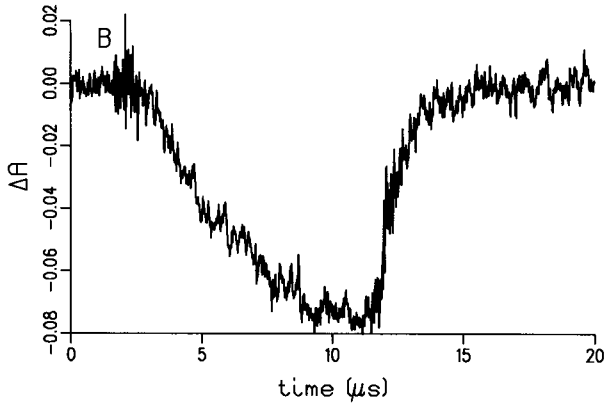

FIGURE 3 Recovered birefringence (*A*) and linear dichroism (*B*) curves of trimeric PS1 using the new method. Results have been calculated from $Z(\alpha)$, with $\alpha = 0.00°$ and $\alpha = \pm 7.95°$. (Sample's optical density: 1.0 at $\lambda = 488$ nm; orienting electric-field strength: 8.5 kV/cm; temperature: 20°C.) The initial positive hump in *A*, when the field is switched on, is caused by the positive birefringence of the buffer.

orientation of the particles (which are more or less disc-shaped with a C3-symmetry axis perpendicular to the plane of the disc (Boekema et al., 1994)) is different for both techniques. In the two-dimensionally compressed gels used for the LD experiments, the axis of symmetry of the molecules will more or less be oriented along the direction in which the gels are compressed, thus perpendicular to the direction of expansion of the gel. Because the electric dichroism is opposite in sign, it can be concluded that the molecules are oriented with their C3-symmetry axis parallel to the applied electric field. This means that the particles must have a permanent electric dipole moment directed parallel to the symmetry axis, causing this axis to become oriented in the direction of the applied field. Sequence analysis combined with structure prediction of the *psa*A-F gene products of PS1 from *Synechocystis* (see Materials and Methods) indicate that PS1

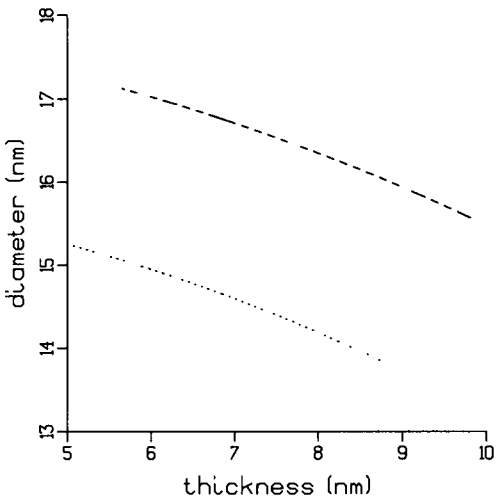

FIGURE 4 Dimensions of PS1 trimers in solutions containing DM and OGP. The lines represent fixed rotational relaxation times (τ) as a function of the thickness and diameter of oblate ellipsoids. The dotted curve (...) represents data from OGP containing solutions (τ = 0.69 μs), the dashed curve (—) indicates results from DM containing solutions (τ = 0.95 μs).

particles possess considerable permanent dipole moments (positive on the lumenal side and negative on the stromal side).

The effect of detergents on the size of PS1 trimers

To investigate the influence of different detergents on the hydrodynamic dimensions of the PS1 particles and as a further check of the method, we also performed TEB measurements on solutions containing the PS1 particle in the detergent OGP and analyzed the birefringence signal in the way as described above. In all cases, the field-free relaxation of the birefringence was found to be mono-exponential and independent of the duration and strength of the applied electric field. When converted to standard conditions (viscosity of water at 20°C), the following exponential relaxation times for the decay of the birefringence were found: τ = 0.95 ± 0.02 μs for PS1 in DM containing buffer, and τ = 0.69 ± 0.02 μs for buffers containing OGP. The indicated errors reflect SDs of the mean from results of mono-exponential fits of at least five birefringence curves.

Because it has not been possible to obtain complete analytical expressions for the rotational properties of short cylinders (discs) (García de la Torre and Bloomfield, 1981), we model trimeric PS1 as oblate ellipsoids. In this way, we can estimate the effect of detergent on the dimensions of PS1 trimers. Fig. 4 shows the results of such an analysis for PS1 in DM- and OGP-containing solutions. Shown are lines of constant rotational correlation time as a function of length and thickness of the oblate ellipsoid. Because trimeric PS1 possesses C3-symmetry around the short axis (Boekema et al., 1994), the decay of the electric-field-induced birefringence will only depend on the rotation of this axis. Therefore, only the rotational correlation time (τ_{ROT}) of the symmetry axis has been calculated using the expressions given by Koenig (1975). Indicated are lines for which τ_{ROT} = 0.95 μs (DM) and τ_{ROT} = 0.69 μs (OGP). If we take the average thickness of PS1 trimers to be 7–8 nm (Boekema et al., 1994), it follows from Fig. 4 that the diameter of the molecule increases from approximately 14.4 to 16.6 nm when OGP is replaced by DM. The value of about 1 nm of the difference in thickness of the detergent layer of DM and OGP is virtually independent of the assumed height of the particle (Fig. 4) and in good agreement with electron microscopy results of Photosystem 2 measured in buffers containing DM and OGP (Dekker et al., 1988). The value of approximately 16.6 nm for the diameter of PS1 trimers in DM is in excellent agreement with recent results obtained from electron microscopy in combination with extensive image analysis (Kruip et al., 1993). This shows that TEB measurement, with the method presented here for separating LD and birefringence effects, provides a sensitive way for the determination of overall structures of these photosynthetic preparations in aqueous solution. The results indicate that the overall structure of trimeric PS1 in solution is not substantially different from that of PS1 under the conditions necessary for electron microscopy.

We are indebted to Prof. S. Aragon for valuable advice to improve the theoretical section. J. Kruip is gratefully acknowledged for calculations on the amino acid sequence of PS1 proteins.

J.P. Dekker was supported by a grant from the Royal Netherlands Academy of Arts and Sciences (KNAW), and M. Rögner was supported by a grant from the Deutsche Forschungsgemeinschaft (DFG).

REFERENCES

Boekema, E. J., A. F. Boonstra, J. P. Dekker, and M. Rögner. 1994. Electron microscopic structural analysis of photosystem I, photosystem II, and the cytochrome *b6/f* complex from green plants and cyanobacteria. *J. Bioenerg. Biomembr.* 26:17–29.

Dekker, J. P., E. J. Boekema, H. T. Witt, and M. Rögner. 1988. Refined purification and further characterization of oxygen-evolving and Tris-treated photosystem II particles from the thermophilic *Cyanobacterium synechococcus* sp. Biochim. Biophys. Acta. 936:307–318.

Fredericq, E., and C. Houssier. 1973. Electric Dichroism and Electric Birefringence. Clarendon Press, Oxford. 219 pp.

Garcïa de la Torre, J., and V. Bloomfield. 1981. Hydrodynamic properties of complex rigid biological macromolecules: theory and applications. *Q. Rev. Biophys.* 14:81–139.

Koenig, S. H. 1975. Brownian motion of an ellipsoid. A correction to Perrin's results. *Biopolymers.* 14:2421–2423.

Krause, S. 1980. Molecular Electro-optics. Plenum Press, New York. 520 pp.

Kruip, J., E. J. Boekema, D. Bald, A. F. Boonstra, and M. Rögner. 1993. Isolation and structural characterization of monomeric and trimeric photosystem I complexes (P700 F_A/F_B and P700 F_X) from the cyanobacterium *Synechocystis* PCC 6803. *J. Biol. Chem.* 268:23353–23360.

Lee, J. van der, D. Bald, S. L. S. Kwa, R. van Grondelle, M. Rögner, and J. P. Dekker. 1993. Steady-state polarized light spectroscopy of isolated photosystem I complexes. *Photosynth. Res.* 35:311–321.

Nordén, B., M. Kubista, and T. Kurucsev. 1992. Linear dichroism spectroscopy of nucleic acids. *Q. Rev. Biophys.* 25:51–170.

O'Konski, C. T. 1978. Molecular Electro-optics. Marcel Dekker, New York. 868 pp.

Provencher, S. W. 1976a. A fourier method for the analysis of exponential decay curves. *Biophys. J.* 16:27–41.

Provencher, S. W. 1976b. An eigenfunction expansion method for the analysis of exponential decay curves. *J. Chem. Phys.* 64:2772–2777.

Ravey, J. C. 1975. Optical anisotropy of absorbing particles: light scattering depolarization, electric- and flow birefringence and dichroism of suspensions of carbon blacks. *Colloid Polymer Sci.* 253:292–305.

Rögner, M., P. J. Nixon, and B. A. Diner. 1990. Purification and characterization of photosystem I and photosystem II core complexes with wild-type and phycocyanin-deficient strains of the cyanobacterium *Synechocystis* PCC 6803. *J. Biol. Chem.* 265:6189–6196.

Tricot, M., and C. Houssier. 1976. Electro-optical properties of synthetic polyelectrolytes. *In* Polyelectrolytes. K. C. Frisch, D. Klempner, and A. V. Patsis, editors. Technomic Publishing, Westport. 43–90.

van Haeringen, B., W. Jiskoot, R. van Grondelle, and M. Bloemendal. 1992. Acid-induced structural changes of a mouse IgG_{2a} monoclonal antibody (MN12) studied by transient electric birefringence measurement. *J. Biomol. Struct. Dyn.* 9:991–1011.

Yamaoka, K., and E. Charney. 1973. Electric dichroism studies of macromolecules in solutions. II. Measurements of linear dichroism and birefringence of deoxyribonucleic acid in orienting electric fields. *Macromolecules.* 6:66–76.

Yoshioka, K., and H. Watanabe. 1969. Dielectric properties of proteins. II. Electric birefringence and dichroism. *In* Physical principles and techniques of protein chemistry. S. J. Leach, editor. Academic Press, New York. 335–367.